Experimental and simulated microplastics transport in saturated natural sediments: impact of grain size and particle size

Wang Li, Giuseppe Brunetti, Christian Zafiu, Marco Kunaschk, Monika Debreczeby, Christine Stumpp

Angaben zur Veröffentlichung / Publication details:

Li, Wang, Giuseppe Brunetti, Christian Zafiu, Marco Kunaschk, Monika Debreczeby, and Christine Stumpp. 2024. "Experimental and simulated microplastics transport in saturated natural sediments: impact of grain size and particle size." *Journal of Hazardous Materials* 468: 133772. https://doi.org/10.1016/j.jhazmat.2024.133772.

Journal of Hazardous Materials 468 (2024) 133772

Contents lists available at ScienceDirect

Journal of Hazardous Materials

journal homepage: www.elsevier.com/locate/jhazmat

Research Paper

Experimental and simulated microplastics transport in saturated natural sediments: Impact of grain size and particle size

Wang Li [a,1,*], Giuseppe Brunetti [a,b], Christian Zafiu [c], Marco Kunaschk [d], Monika Debreczeby [e], Christine Stumpp [a]

[a] University of Natural Resources and Life Sciences, Vienna, Department of Water, Atmosphere and Environment, Institute of Soil Physics and Rural Water Management, Muthgasse 18, 1190 Vienna, Austria
[b] University of Calabria, Department of Civil Engineering, Rende, Italy
[c] University of Natural Resources and Life Sciences, Vienna, Department of Water, Atmosphere and Environment, Institute of Waste Management and Circular Economy, Muthgasse 18, 1190 Vienna, Austria
[d] Bavarian Environment Agency (LfU), Demollstrasse 31, 82407 Wielenbach, Germany
[e] University of Natural Resources and Life Sciences, Vienna, Department of Applied Genetics and Cell Biology, Institute of Molecular Plant Biology, Muthgasse 18, 1190 Vienna, Austria

HIGHLIGHTS

- Mobility of MPs increased with increased sediment size and decreased particle size.
- Breakthrough curve and retention profile are needed for understanding MPs deposition mechanism.
- Simple attachment-detachment model fit well for small microplastics (MPs) (highest R^2).
- Straining plays a significant role in determining the deposition of large MPs in fine sediments.

GRAPHICAL ABSTRACT

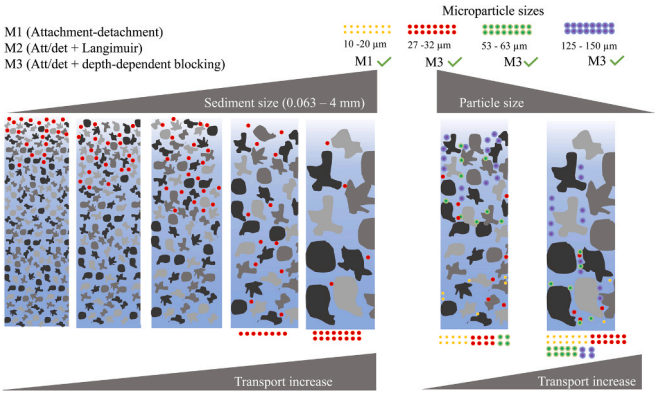

ARTICLE INFO

Keywords:
Microplastics
Sediments
Transport
HYDRUS-1D
Groundwater

ABSTRACT

Microplastics (MPs) present in terrestrial environments show potential leaching risk to deeper soil layers and aquifer systems, which threaten soil health and drinking water supply. However, little is known about the environmental fate of MPs in natural sediments. To examine the MPs transport mechanisms in natural sediments, column experiments were conducted using different natural sediments and MPs (10–150 μm) with conservative tracer. Particle breakthrough curves (BTCs) and retention profiles (RPs) were numerically interpreted in HYDRUS-1D using three different models to identify the most plausible deposition mechanism of MPs. Results show that the retention efficiency for a given particle size increased with decreasing grain size, and RPs exacerbated their hyper-exponential shape in finer sediments. Furthermore, the amounts of MPs present in the

* Corresponding author.
E-mail address: wang.li@boku.ac.at (W. Li).
[1] ORCID: 0000-0002-7298-5836.

https://doi.org/10.1016/j.jhazmat.2024.133772
Received 14 November 2023; Received in revised form 12 January 2024; Accepted 9 February 2024
Available online 10 February 2024

effluent increased to over 85 % as MPs size decreased to 10–20 μm in both gravel and coarse sand columns, while all larger MPs (125–150 μm) were retained in the coarse sand column. The modeling results suggested that the blocking mechanism becomes more important with increasing particle sizes. In particular, the attachment-detachment without blocking was the most suited parameterization to interpret the movement of small MPs, while a depth-dependent blocking approach was necessary to adequately describe the fate of larger particles.

1. Introduction

It was estimated that 12 Gt of plastic waste will end up in the environment by 2050 [23]. Plastic debris in the environment can be broken down and degraded into microplastics (MPs, < 5 mm) and nanoplastics (NPs, 1–1000 nm) (Chain (CONTAM), 2016). Its occurrence in the environment is not limited to marine systems only [14], but is of concern for terrestrial and other aquatic ecosystems [19], too. MPs accumulated in agriculture or found in rivers can enter groundwater bodies and affect directly or indirectly its water quality. This is of particular concern as groundwater is one of the most important drinking water resources worldwide [70], requiring a solid understanding of the fate of MPs in sediments. To date, MPs in groundwater have been detected with variable concentrations within different aquifers, from < 0.7 MP/m^3 to 40 MP/L [42,45]. Although the particles are probably of little concern themselves, they are potential adsorbents of pollutants, such as pesticides [32], heavy metals [37], and antibiotics [62]. Furthermore, additives incorporated in plastic can be released and impair groundwater quality [12]. Additionally, sediments act as the major sink of MPs in the aquatic environment. MPs accumulated in sediments can potentially contaminate aquifer systems through leaching and surface-subsurface interaction in the hyporheic zone [18,5]. River bank filtration has been widely applied in managed aquifer recharge for drinking water supply in Europe [52]. And sand filtration has been suggested as a cost-effective approach for removing MPs from wastewater effluent [22,4,46]. Therefore, a thorough understanding of MPs' deposition mechanism in sediments is essential to assess the environmental fate of MPs in natural systems.

MPs/NPs have been applied as tracers to investigate the transport behavior of colloids or bacteria [13,31,7]. It has been discussed that the deposition of colloids in porous media is attributed to the van der Waals force, hydrodynamic interaction, and electrical double layer [21]. Additionally, sorption of colloids was found to decrease exponentially with depth according to the traditional attachment theory [54]. Column experiments were conducted to examine the influence of physiochemical factors (particle size, grain size, water chemistry, input concentration, and flow rate) on particle transport in porous media [9,7,8]. However, compared to colloids, MPs have a wide size range and many diverse properties (polymer type, surface charge, changed properties due to aging, etc), which potentially impact their fate in sediment, and makes it difficult to assess their pollution risk. To date, the mobility of MPs within natural sediment remains unclear. Current knowledge on MPs' transport in porous media is limited to artificial homogeneous porous media e.g. glass beads [59] or highly purified quartz sand using strong acid [25,26]. Experiments using acid-wash processed sand could change the surface roughness, thus changing the deposition rate [48]. It was reported that heterogeneous surface charge [58], surface roughness [50,55] and collector-particle interaction [56] also play a role in determining MP mobility. In addition, Johnson et al. [28] argued that as the porous media (glass beads, quartz sands) was highly purified with strong acids, this mitigates the possibility of physical-chemical interaction between colloids and porous media, thus ensuring straining as the dominant mechanism for the retention of colloids. Therefore, the transport ability of MPs in natural sediments needs further investigation.

The sediment grain size was found to be the significant factor controlling the transport behavior of MPs. Moreover, greater microsphere mass retention was demonstrated with decreasing grain size of collector for a given input concentration [16,25]. A similar conclusion was reported by Ref. [26] about the mobility of polymer-coated silver nanoplastics, where the mobility of NPs increased with increased grain sizes of quartz sand. And this was further predicted by the colloid filtration theory. It seems possible that these results are due to the decreased retention locations and surface area with increasing collector size. Contrary to this finding, no obvious impact of grain size on sodium dodecylbenzene sulfonate dispersed single-walled nanotubes was observed under both saturated and unsaturated conditions [53]. Therefore, this discrepancy indicates that further in-depth research about grain size impact is still needed, to better understand the retention process of MPs in porous media.

In addition, particle sizes were reported as another dominant factor controlling the mobility of MPs. Column experiments were conducted to investigate the size-dependent transport of microspheres under saturated conditions [17,59,62]. Results in these studies showed increased transport of MPs with decreasing particle size. However, RPs were missing in previous studies [25,31,60,65], which is essential for understanding the retention mechanism and reliable environmental risk [6]. Studies focusing on MPs movement in heterogenous porous media remain scarce, especially with model analysis from both breakthrough curves BTCs and retention profiles RPs [7]. Moreover, considering the broad diversity of MPs in type and size, many of the previous studies use either relatively small MPs (around 1 to 3 μm) or large microplastics (up to mm), despite the fact that a wide size range of existing MPs has been found in the environment. Hence, further research is needed to get a comprehensive understanding of the transport fate of MPs including its retention and testing size ranges abundant in the environment.

Classical colloid filtration theory (CFT) has been widely and successfully used to predict particle retention in porous media under favorable conditions (particle and collector are oppositely charged) [57]. However, there is poor agreement between observation and simulation with CFT observed, which was conducted at low ionic strength with repulsive interaction energy exist (unfavorable attachment condition) [56]. It was pointed out that the discrepancy between experimental observation and CFT model prediction may refer to the lack of consideration of the straining involved in the process [30,41]. In these cases, a two-site transport model with straining considered was found to provide a better description of particle transport behavior [40,71,10]. Though the particle size and grain size impact on particle transport has been recognized, their combined impact on MPs transport and the retention mechanism of MPs in porous media, especially in natural sediments, has received little attention [10,11]. Without comprehensive knowledge on MPs transport mechanism in porous media, it's hard to develop an appropriate model for predicting the migration depth of MPs in sediment or soil, which then also could be a challenge for assessing the potential leaching risk of MPs to groundwater.

Therefore, the main aim of this study is to advance the current understanding of sediment size-dependent MPs mobility under saturated conditions. In particular, the main objectives are: (1) to experimentally examine the impact of particle size and grain size on polyethylene MPs transport (PE MPs) in porous media under saturated conditions; (2) to identify main deposition mechanisms and (3) to quantify transport parameters using different numerical flow and transport models. Small-sized MPs (10–150 μm) were applied in this study, as it was reported as more abundant in the environment but less well-studied. Natural sediments collected from Germany without further purification process were used as porous media. HYDRUS-1D was used to simulate the

observed tracer and MP concentrations in the leachate and the sediment column testing three model concepts to identify the most plausible transport and retention mechanism. It is important to emphasize that only a few studies have used both, breakthrough curve and retention profile data, in the model calibration to examine the fate and retention mechanism of MPs in porous media. Hence, the results of this study could improve the understanding of MPs' transport mechanism and provide valuable information for predicting the leaching risk of MPs in a saturated water environment.

2. Materials and methods

2.1. Experimental setup and analytical methods

2.1.1. Analytical methods

Fluorescent PE microspheres (10–20 μm, 27–32 μm, 53–63 μm, 125–150 μm) were purchased from Cospheric LLC (Santa Barbara, CA, USA) with densities of 0.99–1.01 g/cm^3. The fluorophore is incorporated homogeneously into the PE matrix as reported by the manufacturer, which is also solvent-resistant. The characterization of PE MPs with Fourier-transform infrared spectroscopy (FTIR, Bruker) is presented in Fig. S1. Saturated NaCl (density ~ 1.2 g/cm^3) was selected as the density separation solution for sediment samples. The zeta potential of MPs (Table S1) was measured with a Zetasizer (Nano-ZW, Malvern Panalytical).

As fluorescent PE MPs are hydrophobic, 0.1 % Tween 20 solution (Sigma-Aldrich) was applied to form suspensions with PE MPs, for uniform input of particles on the sediment surface. Stock MP suspensions were prepared by weighing 8 mg of PE MPs (input concentration: 0.005 %, w-w) into 2 mL glass tubes then stirred for 5 min to avoid possible aggregates before injection.

2.1.2. Sediments

Sediments were collected from a gravel pit in Bruckmühl (Germany), air-dried in the oven and sieved into different fractions without further purification process. Speccifically, gravel (G, 2–4 mm), coarse sand (CS, 0.63–2 mm), medium sand (MS, 0.2–0.63 mm), fine sand (FS, 0.063–0.2 mm), and sandy soil (SS, < 2 mm, with 70.3 % medium sand) were used as porous media (Table S1). The first set of columns were packed with sediments of different grain sizes (from G to SS) individually and injected with MPs in the range 27–32 μm, to assess the influence of grain size on MPs mobility. MPs of different sizes (10–20 μm, 53–63 μm, 125–150 μm) were injected in a second set of columns filled with gravel or coarse sand sediments to better understand MP mobility as function of MP size. Duplicate columns were set for each treatment, thus in total, 22 column experiments were conducted to investigate the transport behavior of MPs in natural sediments.

2.1.3. Column experiments

Polymethyl methacrylate columns were used to investigate tracer and MPs transport in saturated porous media. Stainless steel wire mesh with an opening of 200 μm (IBS GES, MBH, Austria) was applied to prevent soil loss from the bottom and to ensure uniform flow distribution at the top. Sediments were weighted and wet-packed to a height of 5 cm. The resulting porosity was 38.7 % for all sediments (known mass of input dry sediments and packed column volume, the density of sediment was set as 2.65 g/cm^3). During packing, the columns were saturated from the bottom and sediment was step-wise filled with avoidance of layering and air entrapment by carefully stirring. Equilibrium conditions were achieved by pumping (peristaltic pump) tap water through columns at a constant flow rate of 1 mL/min (0.73 m/d) in a downward direction. Deuterated water (2 mL, 49.29 mg/L) was applied as a conservative tracer to investigate the conservative transport properties of the packed columns. MPs and tracer were applied as a dirac pulse. A fraction collector with 25 mL glass vials was applied to collect leachates from the outflow for further analysis of tracer and MPs. Tracer samples were analyzed with Cavity Ring-Down Spectrometer Picarro L2130-i Isotope analyzer with a precision of ± 1 ‰ for δ^2H. All the samples were measured 11 times to eliminate the memory effect. The tracer concentration is normalized to the inject concentration C_0 and then plotted as a function of time.

MPs effluent samples were filtrated using Whatman polycarbonate membranes (25 mm diameter, 8 μm pore size, Sigma-Aldrich), which was then measured with a fluorescent microscope (Axio Imager2, ZEISS). Column experiments for tracer and MPs were run for 140 min individually. Afterwards, sediments were sampled per 1 cm-thick layers and transferred into a 250 mL glass beaker. Then 200 mL saturated NaCl and 2 mL hydrogen peroxide H_2O_2 (30 %, Sigma-Aldrich) were added into the beaker, and stirred for 10 min to ensure density separation efficacy. Mixtures were settled for 24 h, and supernatants were collected, the whole process was repeated 3 times to extract all MPs from sediments. Collected supernatant was filtrated with a 0.45 μm regenerated cellulose filter (47 mm diameter, 0.45 μm pore size) by a vacuum pump, which was then further analyzed with confocal laser scanning microscope (SP8, Leica). A schematic diagram of the experimental setup can be found in SI (Fig. S2).

2.1.4. Mass balance

The mass balance of PE MPs was determined by the amount detected in both leachates and sediment segments. The recovery rate was normalized based on the detected particle amounts in samples and injected mass. After soil sampling, the columns were washed with water, and effluent was collected to minimize the loss of MPs adsorbed on the column wall. For the modelling, the mass balance was adjusted by assuming that the MPs' mass balance error primarily occurred in the analysis of the leachate. Therefore, the measured concentration of MPs in effluent was multiplied by $(1\text{-}M_s)/M_{eff}$ to account for the mass balance errors; where M_s and M_{eff} are the measured particle mass fraction in the sediment and effluent, respectively. The average value of results from the duplicate columns was applied for modeling.

2.2. Modeling theory

2.2.1. Tracer transport

The one-dimensional advection-dispersion equation (ADE) was applied to simulate the transport of the conservative tracer. Based on Darcy's law and data from a constant head experiment, the hydraulic conductivity was determined as 0.051 cm/min. The dispersivity was optimized by inverse modeling in HYDRUS 1D [51]. For tracer transport, concentration flux boundary condition and zero concentration gradient were selected as upper and lower boundary conditions. The equation for tracer transport under steady-state flow with constant head can be written as:

$$\frac{\partial C}{\partial t} = -\nu\frac{\partial C}{\partial x} + D_L\frac{\partial^2 C}{\partial^2 x}\# \quad (1)$$

Here C is the tracer concentration in the liquid phase [mL^{-3}], t is time [T,], x is the flow length [L], v is the pore water velocity [LT^{-1}], D_L is the longitudinal dispersion coefficient [L^{2}T^{-1}] with

$$D_L = \alpha_L v\# \quad (2)$$

α_L is the dispersivity [L], which was then used as input value to model the BTCs of MPs.

2.2.2. Microplastics transport

Numerical simulation was conducted to understand the retention mechanism of MPs. In particular, three modified models based on ADE were supplemented to account for MPs' transport. For all model applications, we assume that there are two kinetic sorption sites for MPs retention, in which the first sorption site accounts for MPs deposition on the sediments. The attachment, detachment model (M1) was applied to

consider the retention of MPs only due to attachment, the sorbed concentration of MPs decreases exponentially with depths. The attachment, detachment, and Langmurian blocking model (M2) [1] was used to consider the decreasing attachment coefficient due to decreased sorption sites. The attachment, detachment, and depth-dependent blocking model (M3) was chosen to account for reduced attachment coefficient with increasing depth. The latter assumes that blocking occurs as deposited MPs cover the surface of porous media, which prevents further attachment [13,44].

The total mass balance equation for all models can be written as:

$$\theta\frac{\partial C}{\partial t}+p_b\frac{\partial S_1}{\partial t}+p_b\frac{\partial S_2}{\partial t}=\theta\left(D_L\frac{\partial^2 C}{\partial x^2}-q\frac{\partial C}{\partial x}\right)\# \quad (3)$$

$$p_b\frac{\partial S}{\partial t}=\theta K_{att}\Psi C \quad -p_b K_{\mathrm{det}}S\# \quad (4)$$

Here θ is the volumetric water content [L^3L^{-3}], C is the MPs concentration in the effluent [M L^{-3}, t is time [T], p_b is the bulk density of packed columns [M L^{-3}], S is the MPs concentration in solid phase [M M^{-1}] (1 and 2 represent two kinetic sorption sites), D_L is the dispersion coefficient [L^2 T^{-1}], x is the distance from column inlet [L], q is the pore water velocity [L T^{-1}]. K_{att} is the first-order attachment coefficient [T^{-1}], K_{det} is the first-order detachment coefficient [T^{-1}]. Ψ is the dimensionless MPs retention function, which is flexible and can be used to describe different blocking phenomenon:

$$\Psi=\frac{S_{\max}-S}{S_{\max}}=\left(1-\frac{S}{S_{\max}}\right)\left(\frac{d_{50}+x}{d_{50}}\right)^{-\beta}\# \quad (5)$$

$S_{\max}$ is the maximum MPs concentration in the solid phase [M M^{-1}], d_{50} is the median diameter of sediments [L], β is the empirical factor that controls the shape of RPs [-].

For the first sorption site, Ψ was set as 1 in all models with the assumption that attachment and detachment dominate the deposition of MPs on clean sediments.

$$p_b\frac{\partial S_1}{\partial t}=\theta K_{att1}C-p_b K_{\mathrm{det1}}S_1\# \quad (6)$$

For the second site, which can be described by Eq. (7). Ψ was defined as 1 in M1. For M2, β was set as 0, Ψ is given as Eq. (8). For M3, β was initially chosen as 0.432 [11] and further optimized (see 2.2.3.), and Eq. (9) for M3

$$p_b\frac{\partial S_2}{\partial t}=\theta K_{att2}\Psi C-p_b K_{\mathrm{det2}}S_2\# \quad (7)$$

$$\Psi=\left(1-\frac{S_2}{S_{\max}}\right)\# \quad (8)$$

$$\Psi=\left(\frac{d_{50}+x}{d_{50}}\right)^{-\beta}\# \quad (9)$$

2.2.3. Parameter estimation and model comparison

The HYDRUS-1D inverse solver [39] was used to calibrate the unknown MPs transport parameters (Table 1), which were estimated by fitting to the observed BTCs and RPs. To evaluate the goodness of model fit, the coefficient of model determination R^2 was checked. Additionally, the Akaike information criterion (AIC) was applied to compare the performance of alternative models [2]. The AIC accounts for both model complexity and model fitness:

$$AIC=-2\ln(L)+K\# \quad (10)$$

K is the number of model parameters. L is the maximized log-likelihood of the model. The AIC can help mimic the overfitting potential of the model used for simulation, as AIC increase with the increasing number of parameters. Therefore, the model with minimum AIC value has the optimal balance between model fitness and model parsimony.

Table 1
Process assumptions for the two kinetic sorption sites of the three tested model complexities M1, M2, and M3 and fitted parameters for each assumption. (attachment and detachment (M1); attachment, detachment, and Langmuir dynamics blocking (M2); attachment, detachment, and depth-dependent retention (M3)).

Model	Process		Fitted parameters
	Site 1	Site 2	
M1	attachment-detachment	attachment-detachment	K_{att1}, K_{det1}, K_{att2}, K_{det2}
M2	attachment-detachment	Langmuirian blocking	K_{att1}, K_{det1}, S_{max2}, K_{att2}, K_{det2}
M3	attachment-detachment	depth-dependent blocking	K_{att1}, K_{det1}, β, K_{att2}, K_{det2}

Additionally, particle detachment was assumed to occur as the tailing effect was observed in the BTCs of tracer and MPs during the grain size experiments. Therefore, K_{det} was simulated for all simulations except for experiment results without BTCs (K_{det} was set as 0).

3. Results and discussion

3.1. Tracer breakthrough curves

Fig. 1a presents the normalized deuterium concentration in the effluent collected from columns packed with gravel (G) and coarse sand (CS). All tracer breakthrough curves were uniform indicating that packed columns with one type of sediment were homogeneous and that transport can be approximated with the ADE. Variations between duplicate columns were considered from the difference in packing, although the same packing technique was applied for all columns. The peak time is different between G and CS, with earlier arrival in G due to relatively larger pores in G compared to CS. A similar trend was found with a delayed peak time in columns packed with fine sediments (Fig. S3).

3.2. Model selection

Total mass balance information of MPs in effluent and solid phase is provided in Table S1. High particle mass recovery (M_T = 89–110 %) in all experiments indicated confident and reliable measurement. The 110 % mass recovery might be due to the conversion between particle mass and particle number, thus the actual input particle number would be slightly different than as calculated. To better understand the deposition mechanism of MPs in porous media, observed results were simulated with various models. Table 2 provides the summary of the fitted parameters and model performance (R^2 and AIC).

All tested models describe the BTCs of the smallest MPs (10–20 μm) in columns packed with gravel (G) well, with $R^2 > 0.99$ (Fig. 2a). The similar AIC value (Table 2) indicates that the simple attachment and detachment model (M1) provides good agreement with the experimental results. Also, the BTCs between the stable tracer and MPs (10–20 μm) were similar indicating similar transport like a conservative tracer (Fig. 1b); even though 13.7 ± 0.3 % of MPs still remained in the sediments indicating sorption as additional process in contrast to the tracer. This observation is consistent with a previous study, which reported that polystyrene nanoplastics (50 nm) show similar behavior as tracers in quartz sand columns [49]. As can be seen from Fig. 2e, the model with depth-dependent blocking function (M3) describes the RP of the smallest MPs in G best compared to M1 and M2. This suggests that simulations in BTCs and RPs are needed to provide more comprehensive insight regarding the distribution pattern of MPs in porous media. As shown in Fig. 2c-d and Fig. 2g-h, with increasing particle size, M1 and M2 failed to reproduce the tailing effect in BTCs and hyper-exponential RPs. Instead, improved agreement with both BTC and RP was observed in simulation with a depth-dependent blocking function (M3). A similar

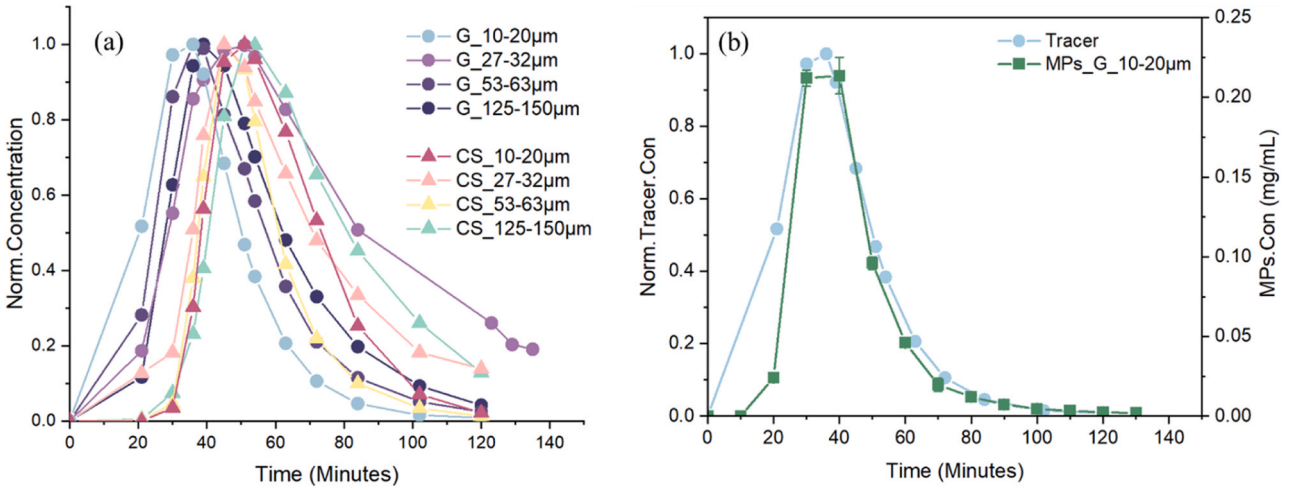

Fig. 1. Observed BTCs of (a) tracer (deuterium) and (b) MPs (10–20 μm) in gravel under the same pulse injection mode and flow velocity. The tracer concentration in (a) is normalized to the inject concentration C_0. G: gravel, CS: coarse sand.

Table 2
Comparison of model performance and summary of fitted parameters with three different models, including attachment and detachment (M1); attachment, detachment, and Langmuir dynamics blocking (M2); attachment, detachment, and depth-dependent retention (M3). (Particle size, d_{MP}; Dispersivity, α_L).

Porous media	d_M μm	α_L cm	Model	K_{att1} min^{-1}	K_{det1} min^{-1}	K_{att2} min^{-1}	K_{det2} min^{-1}	S_{max2}/β mg mg^{-1}	R^2	AIC
Gravel	10-20	0.22	M1	3.59E-03	2.92E-03	3.59E-03	2.92E-03	-	0.995	-139.5
			M2	3.66E-03	2.66E-03	3.51E-03	3.19E-03	1.00E+02	0.995	-137.5
			M3	2.86E-03	3.23E-03	4.36E-03	2.72E-03	5.91E-03	0.995	-137.5
	27-32	0.21	M1	7.81E-03	4.84E-03	7.81E-03	4.84E-03	-	0.986	-121.1
			M2	7.69E-03	5.01E-02	1.09E-02	9.32E-06	2.50E+01	0.997	-146.9
			M3	9.67E-03	6.56E-02	1.39E-02	3.45E-04	9.44E-02	0.999	-171.3
	53-63	0.21	M1	4.87E-02	8.94E-09	4.87E-02	3.96E-03	-	0.867	-80.1
			M2	4.54E-02	6.71E-08	4.54E-02	2.88E-03	2.21E+00	0.876	-71.2
			M3	2.59E-02	1.07E-01	6.31E-01	2.77E-04	1.12E+00	0.998	-152.3
	125-150	0.23	M1	1.11E-01	1.15E-03	1.08E-02	2.86E-04	-	0.746	-67.4
			M2	1.16E-01	1.26E-03	1.72E-02	3.91E-06	5.50E+01	0.758	-64.1
			M3	1.29E-01	2.19E-04	1.38E-01	2.07E-01	3.32E-02	0.980	-112.4
Coarse Sand	10-20	0.21	M1	2.33E-01	1.98E+00	9.28E-03	5.04E-04	-	0.968	-105.9
			M2	9.52E-03	4.84E-04	1.74E-01	1.46E+00	1.00E+03	0.968	-103.9
			M3	4.12E-03	4.48E-06	8.80E-03	1.84E-02	1.80E-02	0.896	-81.7
	27-32	0.19	M1	2.80E-02	4.88E-05	2.84E-02	2.85E-02	-	0.840	-76.2
			M2	2.30E-02	1.99E-02	2.32E-02	6.05E-06	4.99E+02	0.806	-62.4
			M3	3.99E-02	1.12E-03	4.23E-01	1.52E+00	1.79E+02	0.976	-108.8
	53-63	0.13	M1	6.88E-02	2.68E-03	6.88E-02	1.40E-07	-	0.172	-36.0
			M2	-	-	-	-	-	-	-
			M3	1.39E-01	3.21E-04	5.41E+00	4.24E+00	1.00E+04	0.989	-122.5
	125-150	0.21	M1	1.68E-01	-	1.68E-01	-	-	1.000	-19.4
			M2	1.42E-01	-	1.97E-01	-	1.00E+06	1.000	-17.7
			M3	3.04E-01	-	6.19E-05	-	1.00E+06	0.999	-17.5
Medium Sand	27-32	0.21	M1	1.58E-01	-	1.58E-01	-	-	1.000	-37.3
			M2	1.13E-01	-	2.01E-01	-	1.00E+04	0.992	-36.7
			M3	4.07E-01	-	4.29E-05	-	-	0.999	-134.9
Fine Sand	27-32	0.21	M1	1.96E-01	-	1.96E-01	-	-	0.988	-15.9
			M2	1.96E-01	-	2.00E-01	-	7.78E+04	0.989	-14.1
			M3	3.47E-01	-	9.63E-07	-	-	0.983	-15.9
Sandy Soil	27-32	0.19	M1	1.67E-01	-	1.67E-01	-	-	1.000	-21.2
			M2	1.73E-01	-	1.63E-01	-	1.00E+04	1.000	-19.5
			M3	2.74E-01	-	3.30E-05	-	-	0.997	-20.4

trend was also observed in coarse sand (Fig. S4). This demonstrates that M3 provides the best descriptions of both BTCs and RPs for larger MPs, particularly capturing the tailing effect well in BTCs. This was supported by high R^2 and low AIC values. Although there are some discrepancies between observed and fitted RPs, this might contribute to the non-uniform particle and pore size distribution and heterogeneities in surface roughness and surface charge of natural sediments used in this study, which has been reported to influence the mobility of MPs [58]. Compared to M3, M1 and M2 tend to underestimate the deposited concentration of MPs in the surface layer (0–2 cm). Improved agreement between experimental data and simulated results with M3 was noticed in finer sediments as well (Figs. 3 and 4). Therefore, M3 describes the BTCs and RPs better than M1 and M2, particularly for larger MPs in finer sediments, and the assumption that the deposition rate of MPs in both sorption sites is independent (M1 and M2) does actually not hold true.

3.3. *Transport of MPs in different sediments*

To understand the impact of grain size on MPs' mobility, the transport behaviors of PE MPs (27–32 μm) at varying textured sediments

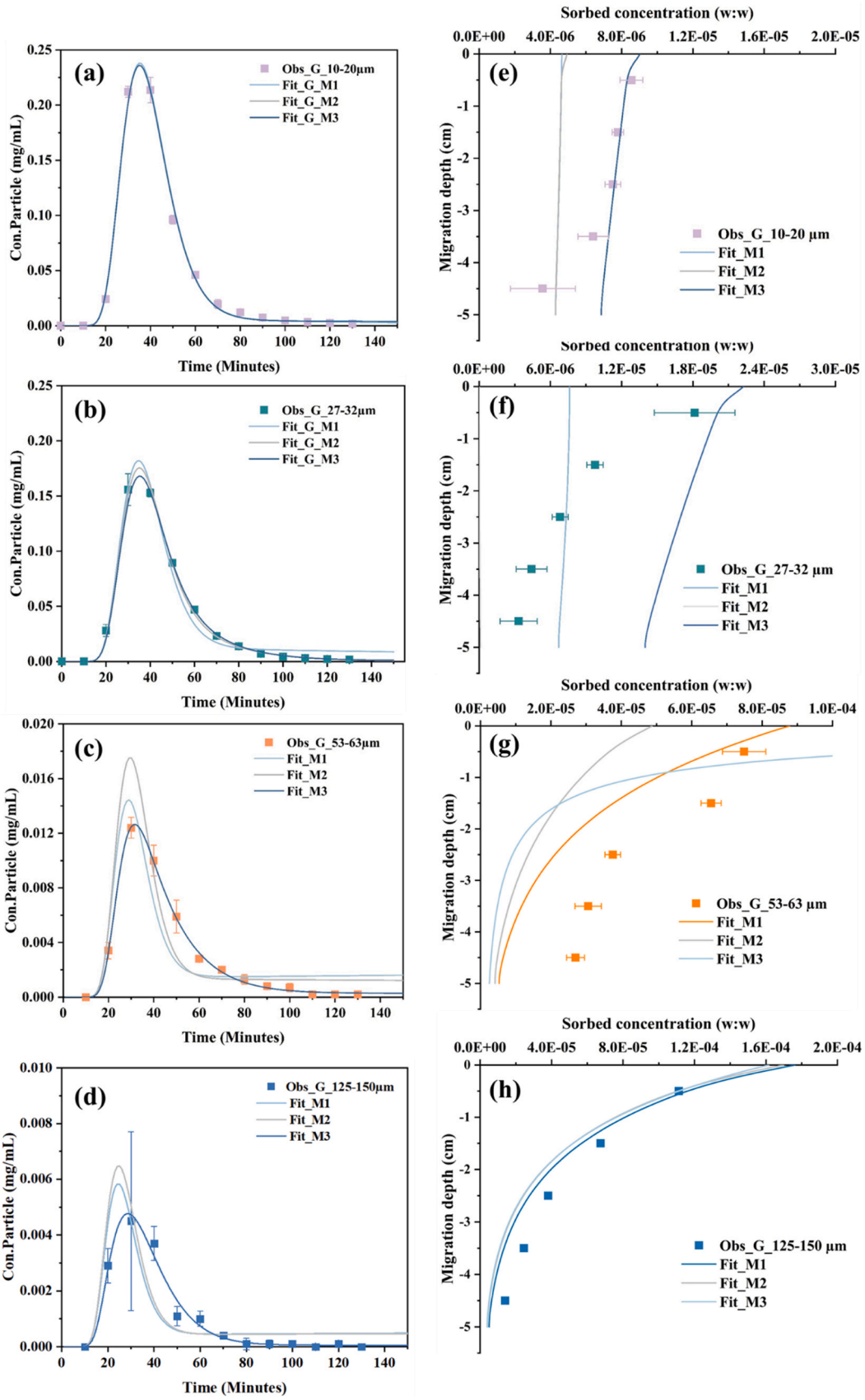

Fig. 2. Effect of particle size (10–150 μm) on the transport of MPs under pulse injection mode in gravel (G). Observed (noted as Obs) and fitted (noted as Fit) breakthrough curves (a-d) and retention profiles (e-h) with three different models including attachment and detachment (M1); attachment, detachment, and Langmuir dynamics blocking (M2); attachment, detachment, and depth-dependent retention (M3). The standard deviation was represented as error bar between duplicate experiments. Note different Y-axis scales in all BTCs and X-axis in all RPs.

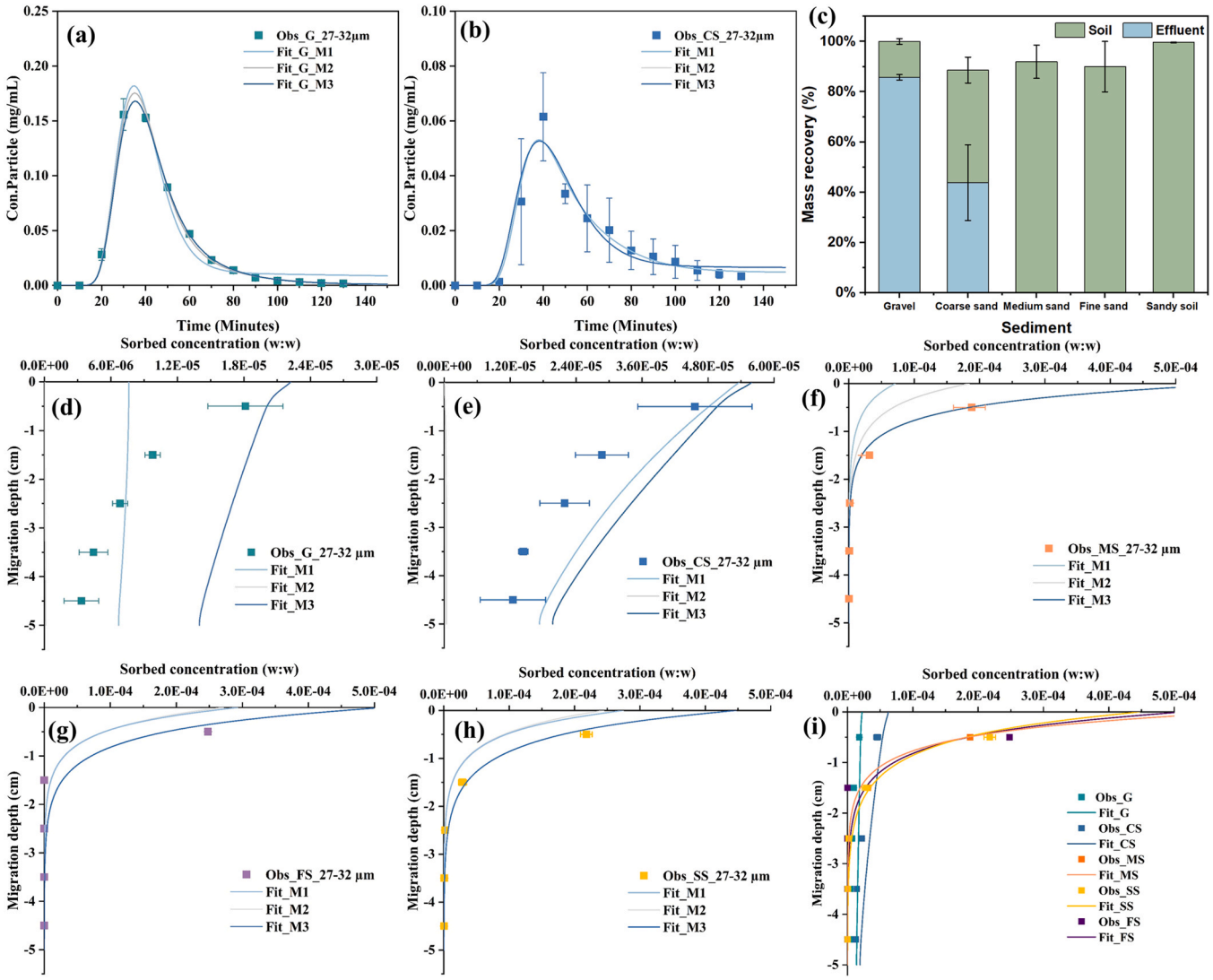

Fig. 3. Observed (scatters, noted as Obs) and fitted (solid lines, noted as Fit) BTCs (a, b) and RPs (d-i) of MPs (27–32 μm) in gravel (G), coarse sand (CS). medium sand (MS), fine sand (FS), and sandy soil (SS) respectively. Summary of mass recovery of MPs in effluent and solid phase (c). Note different Y-axis scales in all BTCs and X-axis in all RPs. The standard deviation was represented as error bars between duplicate experiments.

(gravel, coarse sand, medium sand, fine sand, sandy soil) under saturated conditions were investigated. The observed and simulated BTCs and RPs with different models are present in Fig. 3, with mass balance data shown in Fig. 3c.

MPs showed higher mobility in the gravel column (G) than in the coarse sand column (CS), with mass percentages presented in the effluent of 85.75 ± 1.14 % and 43.82 ± 15.06 %, respectively (Table S1). All MPs were deposited in the columns with fine sediments, and no PE MPs were detected in the effluent collected from columns with medium sand (MS), fine sand (FS), and sandy soil (SS). This suggests that finer sediments contribute to the increased deposition of 27–32 μm PE MPs. Similarly, no BTCs of carboxylated PS MPs were reported in other fine sands [30]. Simulation with M3 (model with a depth-dependent blocking function) in HYDRUS-1D describes the observed BTCs and RPs well, which was further verified with high R^2 (> 0.98) and lower AIC values (Table 2). The decrease of PE MPs in the effluent was consistent with the changes in the K_{att} (Fig. 4e); K_{att1} in the CS (3.99×10^{-2} min^{-1}) was greater than in G (9.67×10^{-3} min^{-1}). This was further confirmed by the accordingly increased K_{det1} in G. Similar results were found in previous experiments showing that the K_{att} of negatively charged latex microspheres (1.0 and 3.2 μm) decreased with increasing grain size for a given input concentration [7]. Compared with the conservative tracer BTCs, earlier peak times of MPs BTCs were noticed in both gravel and coarse sand columns (Fig. S5), indicating that size exclusion is important here. Due to their size, MPs can be excluded from small pores, resulting in transport through larger pores only, and thus an apparent earlier detection peak in the effluent compared to the tracer peak. Similar observations were reported in studies on MPs, bacteria, and viruses transport in soil and/or sediments [31,3].

The observed and fitted RPs with M3 of MPs (27–32 μm) within different sediments (from gravel to sandy soil) are presented in Fig. 3i. For a given MPs size, the RPs tend to be more hyper-exponential in finer texture with most MPs deposited in the inlet of the column, which was also observed by previous lab studies [8,34,33]) as well as a field investigation by (Liu et al., 2018) who found that more MPs were observed in the topsoil (0–3 cm) collected from 20 agricultural fields. Given the grain size is the only change in this set of experiments, the main explanation is that the pore size is smaller in finer sediments inhibiting the transport of MPs due to the reduced pore size and increased retention sites. Hence, the majority of MPs were trapped near the inlet of the column. This indicates that the grain size of porous media plays a significant role in determining the transport fate of MPs under saturated conditions: fine sediments (<0.63 μm) can be employed to remove MPs (27–32 μm) under tested flow velocity. This finding is

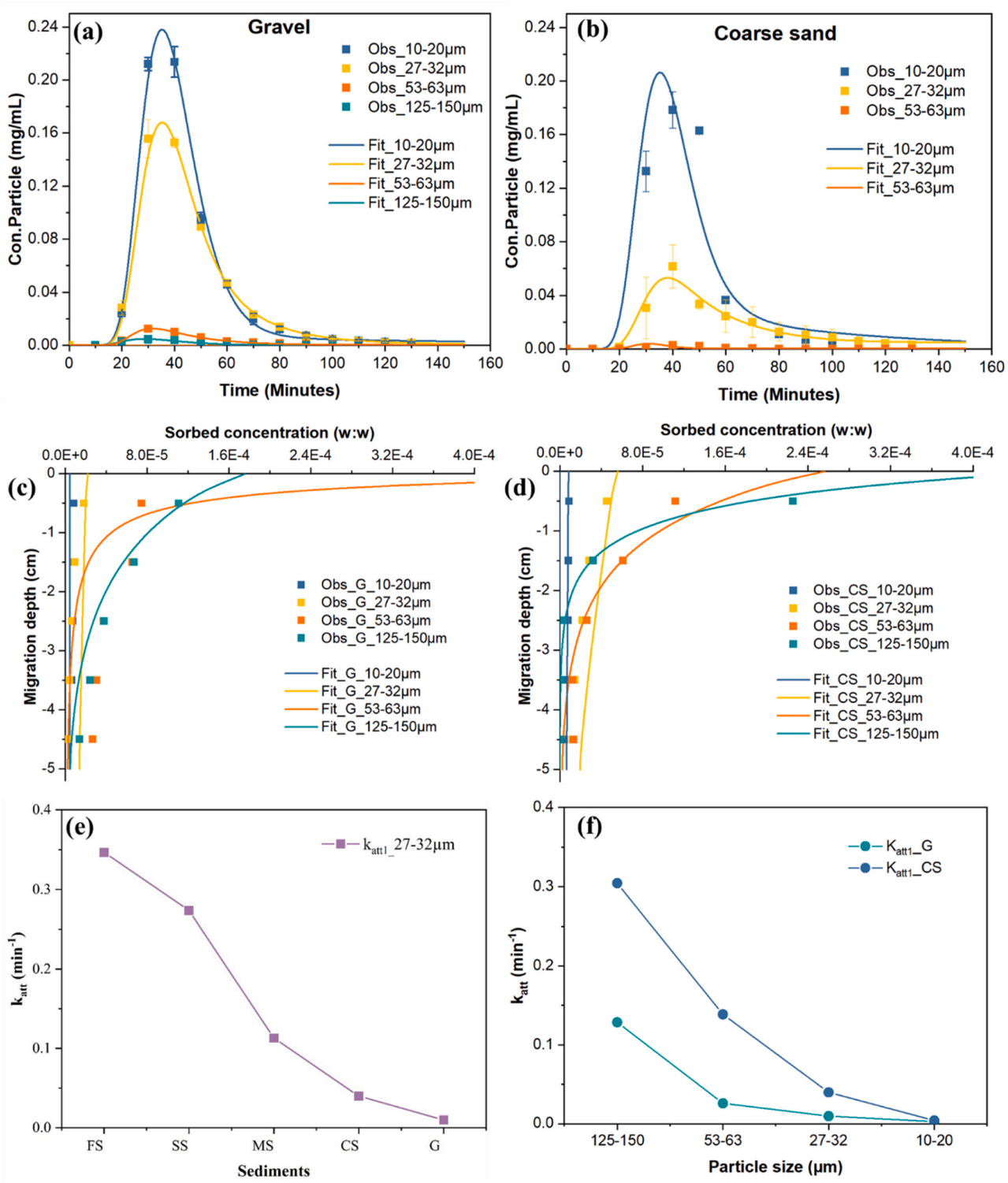

Fig. 4. The observed (scatters) and fitted (solid lines) BTCs (a, b) and RPs (c, d) with M3 of MPs (10–20 μm, 27–32 μm, 53–63 μm, 125–150 μm) in gravel (G), coarse sand (CS). Plot of fitted K_{att1} with M3 for MPs (27–32 μm) in different sediments (e), and MPs (10–20 μm, 27–32 μm, 53–63 μm, 125–150 μm) in gravel (G) and coarse sand (CS) (f).

consistent with the previous study conducted by Hou et al. [25], which suggested that the mobility of PE MPs is positively correlated with the size of quartz sand. However, the mobility of PE MPs (27–32 μm) in this study (M_E = 85 %) is higher than in earlier research, in which PE MPs (40–48 μm) were used, and less MPs (M_E = 75 %) were present in the effluent under the same flow rate (1 mL/min) in gravel (2–4 mm) [25]. Despite the fact that the particle size (27–32 μm) in this experiment is smaller, this could be also attributed to the different column lengths, which were not reported in the previous study [25].

It was demonstrated that straining occurs when the pore throats are too small to allow MPs to pass through. This process was found to be important for the retention of particles when its size was larger than 5 % of the grain size of porous media (McDowell-Boyer et al., 1986). The possibility of straining was determined by the particle-to-grain size ratio

(d_{MP}/d_{50}), which is 0.01, 0.022, 0.069, 0.082, and 0.222, in G, CS, MS, SS, and FS, respectively. Therefore, straining needs to be considered as the responsible mechanism for the increased deposition of MPs in MS, SS, and FS, as straining increased with decreasing grain size of sediments [9]. Improved model performance with M3 in RPs further supports this finding (Fig. 3e-h). Moreover, PE MPs used in this experiment are negatively charged (Table S1), likewise natural sediments also have a negative charge [61]. Thus, existing electrostatic repulsion inhibits the interaction between MPs and porous media. As suggested by [68] the contribution of physicochemical deposition for the retention of MPs can be negligible when the ratio of d_{MP}/d_{50} is larger than 0.005. However, the sediments applied here were not purified, and shape, roughness and pore size were not measured. These were reported to affect the deposition pattern of microsphere under unfavorable conditions [34]. Thus, we considered the contribution of both physicochemical deposition and straining to determine MPs deposition. This also indicates the filtration theory is not appropriate for describing the retention profile in this work, as straining played an important role in MPs deposition, but was not counted in CFT [11]. Specifically, PE MPs were only detected in the first 1 cm in FS, which suggests that FS could be used as filter media to remove MPs from water in wastewater treatment or for water purification in general, like it was suggested in combination with the use of limestone or biochar in other studies [27,35]. Therefore, sand filtration can help to retain large MPs and, thus lower the risk for exposure to large MPs for living organisms in water body. It is assumed that this holds true for MPs of other shapes (such as fragments, pellets, and fibers) too, as spherical MPs have even higher mobility compared to other shapes [29, 59].

3.4. Size-dependent transport of MPs in porous media

The second set of column experiments was conducted to investigate the joint influence of particle size and grain size on MP transport. Observed and simulated BTCs and RPs with M3 are presented in Fig. 4 comparing the transport of four-sizes of MPs (10–20 μm, 27–32 μm, 53–63 μm, 125–150 μm) in G and CS. These results show that the mobility of MPs was sensitive to the change of particle size in a given input concentration, and the maximum effluent concentration of MPs decreased dramatically with increasing particle sizes (Fig. 4a and b). This finding is consistent with that of Ma et al., [38] who also found increased peak concentration of PS microspheres from 16 μm to 3 μm under constant flow condition. Additionally, the released percentage of MPs in effluent decreased with size fractions from 85.27 % for the 10–20 μm fraction to 28.5 % for the 125–150 μm fraction in the gravel column, and no BTCs were observed with MPs at 125–150 μm in the coarse sand column. This observation agreed with the RPs (Fig. 4c and d); there was an increase in retention of MPs with increasing particle size and grain size. Moreover, with increasing particle size, the majority of MPs deposited in the topsoil layer, thus potentially altering its structure and hydraulic properties[64]. In particular, soil water holding capacity and saturated hydraulic conductivity can be altered due to the combined effects of pores' clogging and MPs' hydrophobicity [43,47,64]. The impact of accumulated MPs in soil systems and its effect on soil physical properties depends on MP concentration [66], size [67] and soil texture [24] though, thus different impact of MPs on soil hydraulic properties has been reported. As a consequence of change in soil water storage, nutrient cycling and microbial processes can be altered, thus affecting soil health [69]. The RPs of larger MPs showed a more hyper-exponential shape, which has been reported in previous research [60,7]. This indicates that straining attributed to the larger amount of large MPs (53–150 μm) retained in the first centimeter from the column inlet, as larger particles can't be transported through some of the pore throats (size exclusion). The possibility of straining was determined by the particle-to-grain size ratio (d_{MP}/d_{50}), which is 0.007, 0.01, 0.02, 0.04 for MPs in 10–20 μm, 27–32 μm, 53–63 μm, 125–150 μm, respectively (Table S1). The ratio for MPs (53–150 μm) is significantly larger than the threshold value (0.005)[11]. Hence, we conclude that blocking is an important mechanism for MPs from 53 μm to 150 μm. This implies that focus on top-layer remediation at contaminated sites can help to control the migration risk of MPs into aquifer systems. In contrast, for smaller MPs (10–20 μm) more than 85 % of MPs were present in the effluent from gravel and coarse sand columns. The high mobility of small MPs observed for these types of sediments (0.63–4 mm) suggests an exposure risk of water resources to MPs pollution and associated chemical contamination that originated from MPs-bound additives and MPs-sorbed pollutants[20]. The same magnitude of K_{att} in both gravel and coarse sand columns (Table 2) further supports it. Similar mass retained of MPs (10–20 μm) in gravel (1.12 mg) and coarse sand column (1.10 mg), with similar retention patterns, suggesting that the retention of tested smallest MPs is independent on the porous grain size. These results are in agreement with earlier research which found that there was a similar transport pattern (deposited MPs amount decreased monotonically with packed column depth) for 1.0 and 0.45 μm carboxyl colloids in various-sized Ottawa sands, with the same magnitude of the particle-to-grain size ratio [9].

A lower maximum effluent concentration of MPs (from 10–150 μm) in the coarse sand column than in the gravel column was observed (Fig. 4b). Moreover, there is a clear trend showing higher peak effluent concentration for smaller MPs in gravel. This result can again be explained due to the enhanced straining with increasing particle size and decreasing grain size. Increased K_{att} (Table 2) with increasing MPs and decreasing grain size was observed, indicating straining dominantly attributes to the retained MPs. This finding is consistent with previous work reported that the ratio of diameters of MPs and porous media is the dominant factor influencing the retention of MPs larger than 1 μm[36]. Furthermore, improved agreement between experimental results and simulation with M3 further supports it. It can be seen from Fig. 4e and Fig. 4f, that the value of K_{att1} for certain MPs size decreased with increased grain size and decreased MPs size (for certain sediment). Recall that the mobility of MPs increased with decreasing grain size of sediments and increasing of particle size. This finding was also reported by Bradford et al. [9]. Additionally, previous study found that the impact of particle size on particle mobility varies between mass-based concentration and particle number-based quantification, in which larger NPs had lower retention ([60] P. on C. in the F [15]; roboDąbroś, Van de Ven [44]; Wang et al. [63]). As shown in Fig. S6, the results of our experiment presented in both concentration units confirmed the impact of particle size, with smaller MPs within the tested particle size range showing higher mobility.

4. Summry and conclusions

The main goal of this study was to investigate the impact of grain size and particle size on MPs' transport in saturated porous media. It was important to combine the information of both, BTCs and RPs, for identifying the importance of different transport processes by using different model simulations in HYDRUS-1D. The results demonstrated that the mobility of MPs increased with decreasing particle size and increasing grain size of sediments. Additionally, for small MPs (10–20 μm), the simple attachment and detachment model was sufficient to simulate the experimental BTCs and RPs well. However, for larger MPs and finer sediments, the blocking function was necessary to consider in the model for describing the retention pattern of MPs well. This indicates that the model selection for assessing the MPs mobility depends on particle size and porous media. In addition, our results highlight the importance of combining BTCs and RPs to get a precise description of MPs' transport behavior. According to the retention profile results, MPs accumulated in sediments are likely to migrate into deeper layers. The high mobility of PE MPs in natural sediments observed in this study suggests a high groundwater pollution risk for those particles and their additives. Hence, more research is needed not only to understand the risks of the MP particles in groundwater but also the chemical additives that are

incorporated into the plastic polymer or persistent pollutants sorbed to the MPs. The observed effect of plastic size on MPs mobility in different grain size sediment can have many environmental implications in water treatment and remediation of polluted systems. In particular, the identified transport parameters can be applied in designing filtration system to improve the retention of different -sized MPs. However, it must be highlighted that the transport of MPs in natural environments is influenced by multiple properties such as shape, surface charge, and hydrophobicity, which were only partially investigated in the present study. Moreover, natural atmospheric conditions (i.e., alternation of drought periods and precipitation) are likely to trigger more complex interplays between MPs and soil, which were not analyzed in this work. Thus, future studies should focus on MPs with different properties, combined with long-term field experiments to understand the fate of MPs in real conditions. Nevertheless, laboratory experiments remain a necessary preliminary step to reduce uncertainties, before evaluating the fate of MP in the field.

Environmental implication

Previous studies examined the fate of microplastics in saturated systems using highly purified artificial porous media. In this paper, we use natural sediments without eliminating the sediment surface impurity to investigate the transport of differently sized microplastics (abundant but rarely tested size range) with low, environmental relevant, concentration. The observed size-dependent impact on the microplastics' mobility indicating higher risk of groundwater to smaller microplastic. In addition, experimental results were further combined with different models to discuss the most plausible deposition mechanism of microplastics. The identified transport parameters can be used in future studies to assess groundwater pollution risks.

CRediT authorship contribution statement

Christine Stumpp: Conceptualization, Funding acquisition, Project administration, Resources, Supervision, Writing – review & editing. **Marco Kunaschk:** Methodology, Writing – review & editing. **Monika Debreczeby:** Methodology, Writing – review & editing. **Giuseppe Brunetti:** Conceptualization, Formal analysis, Methodology, Writing – review & editing. **Christian Zafiu:** Methodology, Writing – review & editing. **Wang Li :** Conceptualization, Data curation, Formal analysis, Investigation, Methodology, Software, Visualization, Writing – original draft, Writing – review & editing.

Declaration of Competing Interest

The authors declare that they have no known competing financial interests or personal relationships that could have appeared to influence the work reported in this paper.

Data availability

Data will be made available on request.

Acknowledgments

We would like to thank Ms. Martina Faulhammer for her help in the lab for isotope measurement, Mr. Wisam Almohamed for lab column setup, MSc Emilee Severe for her assistance in revising the English in the manuscript The confocal laser scanning microscopy (SP8, Leica) was kindly provided by the BOKU Core Facility Multiscale Imaging. This study was supported by the project SOPLAS, which has received funding from the European Union's Horizon 2020 Research and Innovation Programme under the Marie Skłodowska-Curie grant agreement No 955334.

Appendix A. Supporting information

Supplementary data associated with this article can be found in the online version at doi:10.1016/j.jhazmat.2024.133772.

References

[1] Adamczyk, Z., Siwek, B., Zembala, M., Belouschek, P., 1994. Kinetics of localized adsorption of colloid particles. Adv Colloid Interface Sci 48, 151–280. https://doi.org/10.1016/0001-8686(94)80008-1.
[2] Akaike, H., 1998. Information theory and an extension of the maximum likelihood principle. In: Parzen, E., Tanabe, K., Kitagawa, G. (Eds.), Selected Papers of Hirotugu Akaike. Springer New York, pp. 199–213. https://doi.org/10.1007/978-1-4612-1694-0_15.
[3] Bales, R.C., Gerba, C.P., Grondin, G.H., Jensen, S.L., 1989. Bacteriophage transport in sandy soil and fractured tuff. Appl Environ Microbiol 55 (8), 2061–2067. https://doi.org/10.1128/aem.55.8.2061-2067.1989.
[4] Bayo, J., Olmos, S., López-Castellanos, J., 2020. Microplastics in an urban wastewater treatment plant: The influence of physicochemical parameters and environmental factors. Chemosphere 238, 124593. https://doi.org/10.1016/j.chemosphere.2019.124593.
[5] Boano, F., Harvey, J.W., Marion, A., Packman, A.I., Revelli, R., Ridolfi, L., et al., 2014. Hyporheic flow and transport processes: Mechanisms, models, and biogeochemical implications. Rev Geophys 52 (4), 603–679. https://doi.org/10.1002/2012RG000417.
[6] Bradford, S.A., Bettahar, M., 2005. Straining, attachment, and detachment of Cryptosporidium oocysts in saturated porous media. J Environ Qual 34 (2), 469–478.
[7] Bradford, S.A., Bettahar, M., 2006. Concentration dependent transport of colloids in saturated porous media. J Contam Hydrol 82 (1), 99–117. https://doi.org/10.1016/j.jconhyd.2005.09.006.
[8] Bradford, S.A., Torkzaban, S., Walker, S.L., 2007. Coupling of physical and chemical mechanisms of colloid straining in saturated porous media. Water Res 41 (13), 3012–3024. https://doi.org/10.1016/j.watres.2007.03.030.
[9] Bradford, S.A., Yates, S.R., Bettahar, M., Simunek, J., 2002. Physical factors affecting the transport and fate of colloids in saturated porous media. Water Resour Res 38 (12). https://doi.org/10.1029/2002WR001340, 63-1.
[10] Bradford, S.A., Bettahar, M., Simunek, J., van Genuchten, M.Th, 2004. Straining and attachment of colloids in physically heterogeneous porous media. Vadose Zone J 3 (2), 384–394. https://doi.org/10.2113/3.2.384.
[11] Bradford, S.A., Simunek, J., Bettahar, M., van Genuchten, M.Th, Yates, S.R., 2003. Modeling colloid attachment, straining, and exclusion in saturated porous media. Environ Sci Technol 37 (10), 2242–2250. https://doi.org/10.1021/es025899u.
[12] Bridson, J.H., Gaugler, E.C., Smith, D.A., Northcott, G.L., Gaw, S., 2021. Leaching and extraction of additives from plastic pollution to inform environmental risk: a multidisciplinary review of analytical approaches. J Hazard Mater 414, 125571.
[13] Camesano, T.A., Unice, K.M., Logan, B.E., 1999. Blocking and ripening of colloids in porous media and their implications for bacterial transport. Colloids Surf A: Physicochem Eng Asp 160 (3), 291–307.
[14] Carpenter, E.J., Anderson, S.J., Harvey, G.R., Miklas, H.P., Peck, B.B., 1972. Polystyrene spherules in coastal waters. Science 178 (4062), 749–750. https://doi.org/10.1126/science.178.4062.749.
[15] Chain (CONTAM), E. P. on C. in the F, 2016. Presence of microplastics and nanoplastics in food, with particular focus on seafood. Efsa J 14 (6), e04501.
[16] Dong, S., Xia, J., Sheng, L., Wang, W., Liu, H., Gao, B., 2021. Transport characteristics of fragmental polyethylene glycol terephthalate (PET) microplastics in porous media under various chemical conditions. Chemosphere 276, 130214. https://doi.org/10.1016/j.chemosphere.2021.130214.
[17] Dong, Z., Qiu, Y., Zhang, W., Yang, Z., Wei, L., 2018. Size-dependent transport and retention of micron-sized plastic spheres in natural sand saturated with seawater. Water Res 143, 518–526. https://doi.org/10.1016/j.watres.2018.07.007.
[18] Drummond, J.D., Nel, H.A., Packman, A.I., Krause, S., 2020. Significance of Hyporheic Exchange for Predicting Microplastic Fate in Rivers. Environ Sci Technol Lett 7 (10), 727–732. https://doi.org/10.1021/acs.estlett.0c00595.
[19] Duis, K., Coors, A., 2016. Microplastics in the aquatic and terrestrial environment: sources (with a specific focus on personal care products), fate and effects. Environ Sci Eur 28 (1), 2. https://doi.org/10.1186/s12302-015-0069-y.
[20] Eder, M.L., Oliva-Teles, L., Pinto, R., Carvalho, A.P., Almeida, C.M.R., Hornek-Gausterer, R., Guimarães, L., 2021. Microplastics as a vehicle of exposure to chemical contamination in freshwater systems: current research status and way forward. J Hazard Mater 417, 125980. https://doi.org/10.1016/j.jhazmat.2021.125980.
[21] Elimelech, M., O'melia, C.R., 1990. Kinetics of deposition of colloidal particles in porous media. Environ Sci Technol 24, 1528–1536.
[22] Funck, M., Al-Azzawi, M.S.M., Yildirim, A., Knoop, O., Schmidt, T.C., Drewes, J.E., Tuerk, J., 2021. Release of microplastic particles to the aquatic environment via wastewater treatment plants: The impact of sand filters as tertiary treatment. Chem Eng J 426, 130933. https://doi.org/10.1016/j.cej.2021.130933.
[23] Geyer, R., Jambeck, J.R., Law, K.L., 2017. Production, use, and fate of all plastics ever made. Sci Adv 3 (7), e1700782. https://doi.org/10.1126/sciadv.1700782.
[24] Guo, Z., Li, P., Yang, X., Wang, Z., Lu, B., Chen, W., Wu, Y., Li, G., Zhao, Z., Liu, G., Ritsema, C., Geissen, V., Xue, S., 2022. Soil texture is an important factor determining how microplastics affect soil hydraulic characteristics. Environ Int 165, 107293. https://doi.org/10.1016/j.envint.2022.107293.

[25] Hou, J., Xu, X., Lan, L., Miao, L., Xu, Y., You, G., Liu, Z., 2020. Transport behavior of micro polyethylene particles in saturated quartz sand: Impacts of input concentration and physicochemical factors. Environ Pollut 263, 114499. https://doi.org/10.1016/j.envpol.2020.114499.
[26] Hou, J., Zhang, M., Wang, P., Wang, C., Miao, L., Xu, Y., You, G., Lv, B., Yang, Y., Liu, Z., 2017. Transport and long-term release behavior of polymer-coated silver nanoparticles in saturated quartz sand: the impacts of input concentration, grain size and flow rate. Water Res 127, 86–95. https://doi.org/10.1016/j.watres.2017.10.017.
[27] Hsieh, L., He, L., Zhang, M., Lv, W., Yang, K., Tong, M., 2022. Addition of biochar as thin preamble layer into sand filtration columns could improve the microplastics removal from water. Water Res 221, 118783. https://doi.org/10.1016/j.watres.2022.118783.
[28] Johnson, W.P., Ma, H., Pazmino, E., 2011. Straining Credibility: A General Comment Regarding Common Arguments Used to Infer Straining As the Mechanism of Colloid Retention in Porous Media. Environ Sci Technol 45 (9), 3831–3832. https://doi.org/10.1021/es200868e.
[29] Knappenberger, T., Aramrak, S., Flury, M., 2015. Transport of barrel and spherical shaped colloids in unsaturated porous media. J Contam Hydrol 180, 69–79. https://doi.org/10.1016/j.jconhyd.2015.07.007.
[30] Knappett, P.S.K., Emelko, M.B., Zhuang, J., McKay, L.D., 2008. Transport and retention of a bacteriophage and microspheres in saturated, angular porous media: Effects of ionic strength and grain size. Water Res 42 (16), 4368–4378. https://doi.org/10.1016/j.watres.2008.07.041.
[31] Kretzschmar, R., Barmettler, K., Grolimund, D., Yan, Y., Borkovec, M., Sticher, H., 1997. Experimental determination of colloid deposition rates and collision efficiencies in natural porous media. Water Resour Res 33 (5), 1129–1137. https://doi.org/10.1029/97WR00298.
[32] Li, H., Wang, F., Li, J., Deng, S., Zhang, S., 2021. Adsorption of three pesticides on polyethylene microplastics in aqueous solutions: Kinetics, isotherms, thermodynamics, and molecular dynamics simulation. Chemosphere 264, 128556. https://doi.org/10.1016/j.chemosphere.2020.128556.
[33] Li, X., Scheibe, T.D., Johnson, W.P., 2004. Apparent decreases in colloid deposition rate coefficients with distance of transport under unfavorable deposition conditions: a general phenomenon. Environ Sci Technol 38 (21), 5616–5625. https://doi.org/10.1021/es049154v.
[34] Li, X., Lin, C.L., Miller, J.D., Johnson, W.P., 2006. Role of grain-to-grain contacts on profiles of retained colloids in porous media in the presence of an energy barrier to deposition. Environ Sci Technol 40 (12), 3769–3774. https://doi.org/10.1021/es052501w.
[35] Li, X., Zhang, Y., Xu, H., Sun, Y., Gao, B., Wu, J., 2023. Granular limestone amended sand filters for enhanced removal of nanoplastics from water: performance and mechanisms. Water Res 229, 119443. https://doi.org/10.1016/j.watres.2022.119443.
[36] Lim, S.J., Seo, J., Hwang, M., Kim, H.C., Kim, E.J., Lee, J., Hong, S.W., Lee, S., Chung, J., 2023. A multi-scale framework for modeling transport of microplastics during sand filtration: Bridging from pore to continuum. J Hazard Mater 443, 130219. https://doi.org/10.1016/j.jhazmat.2022.130219.
[37] Liu, S., Huang, J., Zhang, W., Shi, L., Yi, K., Zhang, C., Pang, H., Li, J., Li, S., 2022. Investigation of the adsorption behavior of Pb(II) onto natural-aged microplastics as affected by salt ions. J Hazard Mater 431, 128643. https://doi.org/10.1016/j.jhazmat.2022.128643.
[38] Ma, E., Ouahbi, T., Wang, H., Ahfir, N.D., Alem, A., Hammadi, A., 2017. Modeling of retention and re-entrainment of mono- and poly-disperse particles: Effects of hydrodynamics, particle size and interplay of different-sized particles retention. Sci Total Environ 596–597, 222–229. https://doi.org/10.1016/j.scitotenv.2017.03.254.
[39] Marquardt, D.W., 1963. An algorithm for least-squares estimation of nonlinear parameters. J Soc Ind Appl Math 11 (2), 431–441. https://doi.org/10.1137/0111030.
[40] Mattison, N.T., O'Carroll, D.M., Kerry Rowe, R., Petersen, E.J., 2011. Impact of porous media grain size on the transport of multi-walled carbon nanotubes. Environ Sci Technol 45 (22), 9765–9775. https://doi.org/10.1021/es2017076.
[41] McDowell-Boyer, L.M., Hunt, J.R., Sitar, N., 1986. Particle transport through porous media. Water Resour Res 22 (13), 1901–1921.
[42] Mintenig, S.M., Löder, M.G.J., Primpke, S., Gerdts, G., 2019. Low numbers of microplastics detected in drinking water from ground water sources. Sci Total Environ 648, 631–635. https://doi.org/10.1016/j.scitotenv.2018.08.178.
[43] Qi, Y., Beriot, N., Gort, G., Huerta Lwanga, E., Gooren, H., Yang, X., Geissen, V., 2020. Impact of plastic mulch film debris on soil physicochemical and hydrological properties. Environ Pollut 266, 115097. https://doi.org/10.1016/j.envpol.2020.115097.
[44] roboDąbroś, T., Van de Ven, T.G.M., 1982. Kinetics of coating by colloidal particles. J Colloid Interface Sci 89 (1), 232–244.
[45] Samandra, S., Johnston, J.M., Jaeger, J.E., Symons, B., Xie, S., Currell, M., Ellis, A. V., Clarke, B.O., 2022. Microplastic contamination of an unconfined groundwater aquifer in Victoria, Australia. Sci Total Environ 802, 149727. https://doi.org/10.1016/j.scitotenv.2021.149727.
[46] Sembiring, E., Fajar, M., Handajani, M., 2021. Performance of rapid sand filter – single media to remove microplastics. Water Supply 21. https://doi.org/10.2166/ws.2021.060.
[47] Shafea, L., Felde, V.J.M.N.L., Woche, S.K., Bachmann, J., Peth, S., 2023. Microplastics effects on wettability, pore sizes and saturated hydraulic conductivity of a loess topsoil. Geoderma 437, 116566. https://doi.org/10.1016/j.geoderma.2023.116566.
[48] Shani, C., Weisbrod, N., Yakirevich, A., 2008. Colloid transport through saturated sand columns: Influence of physical and chemical surface properties on deposition. Colloids Surf A: Physicochem Eng Asp 316 (1), 142–150. https://doi.org/10.1016/j.colsurfa.2007.08.047.
[49] Shaniv, D., Dror, I., Berkowitz, B., 2021. Effects of particle size and surface chemistry on plastic nanoparticle transport in saturated natural porous media. Chemosphere 262, 127854. https://doi.org/10.1016/j.chemosphere.2020.127854.
[50] Shen, C., Wang, L.P., Li, B., Huang, Y., Jin, Y., 2012. Role of surface roughness in chemical detachment of colloids deposited at primary energy minima. Vadose Zone J 11, 1.
[51] Simunek, J, Jirka, Saito H, Sakai M, Van Genuchten M. The HYDRUS-1D software package for simulating the one-dimensional movement of water, heat, and multiple solutes in variably-saturated media; 2008.
[52] Sprenger, C., Hartog, N., Hernández, M., Vilanova, E., Grützmacher, G., Scheibler, F., Hannappel, S., 2017. Inventory of managed aquifer recharge sites in Europe: Historical development, current situation and perspectives. Hydrogeol J 25 (6), 1909.
[53] Tian, Y., Gao, B., Ziegler, K.J., 2011. High mobility of SDBS-dispersed single-walled carbon nanotubes in saturated and unsaturated porous media. J Hazard Mater 186 (2–3), 1766–1772.
[54] Tobiason, J.E., O'melia, C.R., 1988. Physicochemical aspects of particle removal in depth filtration. J Water Works Assoc 80 (12), 54–64.
[55] Torkzaban, S., Bradford, S.A., 2016. Critical role of surface roughness on colloid retention and release in porous media. Water Res 88, 274–284.
[56] Tufenkji, N., Elimelech, M., 2004. Deviation from the classical colloid filtration theory in the presence of repulsive DLVO interactions. Langmuir 20 (25), 10818–10828.
[57] Tufenkji, N., Elimelech, M., 2004. Correlation equation for predicting single-collector efficiency in physicochemical filtration in saturated porous media. Environ Sci Technol 38 (2), 529–536.
[58] Tufenkji, N., Elimelech, M., 2005. Breakdown of colloid filtration theory: Role of the secondary energy minimum and surface charge heterogeneities. Langmuir 21 (3), 841–852.
[59] Waldschläger, K., Schüttrumpf, H., 2020. Infiltration behavior of microplastic particles with different densities, sizes, and shapes—From glass spheres to natural sediments. Environ Sci Technol 54 (15), 9366–9373.
[60] Wang, C., Bobba, A.D., Attinti, R., Shen, C., Lazouskaya, V., Wang, L.P., Jin, Y., 2012. Retention and transport of silica nanoparticles in saturated porous media: Effect of concentration and particle size. Environ Sci Technol 46 (13), 7151–7158.
[61] Wang, F., Chen, J., Chen, J., Forsling, W., 1997. Surface properties of natural aquatic sediments. Water Res 31 (7), 1796–1800.
[62] Wang, K., Han, T., Chen, X., Rushimisha, I.E., Liu, Y., Yang, S., Miao, X., Li, X., Weng, L., Li, Y., 2022. Insights into behavior and mechanism of tetracycline adsorption on virgin and soil-exposed microplastics. J Hazard Mater 440, 129770. https://doi.org/10.1016/j.jhazmat.2022.129770.
[63] Wang, Y., Xu, L., Chen, H., Zhang, M., 2022. Retention and transport behavior of microplastic particles in water-saturated porous media. Sci Total Environ 808, 152154.
[64] Wang, Z., Li, W., Li, W., Yang, W., Jing, S., 2023. Effects of microplastics on the water characteristic curve of soils with different textures. Chemosphere 317, 137762. https://doi.org/10.1016/j.chemosphere.2023.137762.
[65] Xi, X., Wang, L., Zhou, T., Yin, J., Sun, H., Yin, X., Wang, N., 2022. Effects of physicochemical factors on the transport of aged polystyrene nanoparticles in saturated porous media. Chemosphere 289, 133239.
[66] Xie, Y., Wang, H., Chen, Y., Guo, Y., Wang, C., Cui, H., Xue, J., 2023. Water retention and hydraulic properties of a natural soil subjected to microplastic contaminations and leachate exposures. Sci Total Environ 901, 166502. https://doi.org/10.1016/j.scitotenv.2023.166502.
[67] Xing, X., Yu, M., Xia, T., Ma, L., 2021. Interactions between water flow and microplastics in silt loam and loamy sand. Soil Sci Soc Am J 85 (6), 1956–1962. https://doi.org/10.1002/saj2.20337.
[68] Xu, S., Gao, B., Saiers, J.E., 2006. Straining of colloidal particles in saturated porous media. Water Resour Res 42, 12.
[69] Yuan, Y., Zu, M., Li, R., Zuo, J., Tao, J., 2023. Soil properties, microbial diversity, and changes in the functionality of saline-alkali soil are driven by microplastics. J Hazard Mater 446, 130712. https://doi.org/10.1016/j.jhazmat.2022.130712.
[70] Zektser, I.S., Everett, L.G., 2000. Groundwater and the environment: applications for the global community. CRC Press.
[71] Zhang, L., Hou, L., Wang, L., Kan, A.T., Chen, W., Tomson, M.B., 2012. Transport of fullerene nanoparticles (n C60) in saturated sand and sandy soil: controlling factors and modeling. Environ Sci Technol 46 (13), 7230–7238.